

Discovery of the True Peroxy Intermediate in the Catalytic Cycle of Terminal Oxidases by Real-time Measurement*

Received for publication, July 6, 2007, and in revised form, August 6, 2007 Published, JBC Papers in Press, August 9, 2007, DOI 10.1074/jbc.M705562200

Ilya Belevich^{†1}, Vitaliy B. Borisov^{§1}, and Michael I. Verkhovsky^{‡2}

From the [†]Helsinki Bioenergetics Group, Institute of Biotechnology, University of Helsinki, Post Office Box 65 (Viikinkaari 1), FI-00014 Helsinki, Finland and [§]Department of Molecular Energetics of Microorganisms, Belozersky Institute of Physico-Chemical Biology, Lomonosov Moscow State University, Moscow 119991, Russia

The sequence of the catalytic intermediates in the reaction of cytochrome *bd* terminal oxidases from *Escherichia coli* and *Azotobacter vinelandii* with oxygen was monitored in real time by absorption spectroscopy and electrometry. The initial binding of O₂ to the fully reduced enzyme is followed by the fast (5 μs) conversion of the oxy complex to a novel, previously unresolved intermediate. In this transition, low spin heme *b*₅₅₈ remains reduced while high spin heme *b*₅₉₅ is oxidized with formation of a new heme *d*-oxygen species with an absorption maximum at 635 nm. Reduction of O₂ by two electrons is sufficient to produce (hydro)peroxide bound to ferric heme *d*. In this case, the O-O bond is left intact and the newly detected intermediate must be a peroxy complex of heme *d* (Fe_d³⁺-O-O-(H)) corresponding to compound 0 in peroxidases. The alternative scenario where the O-O bond is broken as in the P_M intermediate of heme-copper oxidases and compound I of peroxidases is not very likely, because it would require oxidation of a nearby amino acid residue or the porphyrin ring that is energetically unfavorable in the presence of the reduced heme *b*₅₅₈ in the proximity of the catalytic center. The formation of the peroxy intermediate is not coupled to membrane potential generation, indicating that hemes *d* and *b*₅₉₅ are located at the same depth of the membrane dielectric. The lifetime of the new intermediate is 47 μs; it decays into oxoferryl species due to oxidation of low spin heme *b*₅₅₈ that is linked to significant charge translocation across the membrane.

Heme enzymes such as peroxidases, catalases, cytochromes P450, and terminal oxidases are suggested to share the key catalytic intermediates, namely peroxy and oxoferryl. Reaction of peroxidases with H₂O₂ suggests sequential formation of a peroxy complex (compound 0, Fe³⁺-OOH), and the two oxoferryl species, compound I (Fe⁴⁺ = O R[•], where R[•] is a porphyrin or amino acid radical) and compound II (Fe⁴⁺ = O) (Ref. 1 and references therein). Compound 0 could be detected at low tem-

peratures (2) but not at room temperature (3). Studies on heme-copper terminal oxidases reported the intermediates analogous to compound I (P_M) and compound II (P_R and F) (4–23). A transient formation of an intermediate equivalent to compound 0 has been proposed but never documented in heme-copper oxidases.

Cytochromes *bd* comprise a peculiar class of terminal oxidases performing a number of vitally important functions in bacteria (Ref. 24 and references therein). Like heme-copper oxidases, cytochrome *bd* conserves energy in the form of electrochemical proton gradient (Δμ_H⁺) across the membrane accumulated in the reaction of the reduction of molecular oxygen to water (25–29). Cytochrome *bd*, however, is not a proton pump (30), and the formation of Δμ_H⁺ occurs only due to the vectorial chemistry where the protons from quinol oxidation are released into the positive (periplasmic) side of the membrane whereas protons required for water formation are taken up from the negative (cytoplasmic) side. Cytochrome *bd* uses ubiquinol or menaquinol, but never cytochrome *c*, as a natural respiratory substrate. Cytochrome *bd* contains three hemes (*b*₅₅₈, *b*₅₉₅, and *d*) but no copper (27). The low spin heme *b*₅₅₈ seems to be directly involved in quinol oxidation, whereas the high spin hemes *b*₅₉₅ and *d* likely form a di-heme catalytic site for binding and activation of O₂, reducing it further to H₂O (31–37).

The reaction of the fully reduced (R^{Footnote}) cytochrome *bd* with oxygen showed the sequential formation of the 650- and 680-nm absorbing species (38, 39). The 680-nm species can also be generated by the addition of excess H₂O₂ to the “as-isolated” or fully oxidized (O)³ form of the enzyme (39–43). The 650- and 680-nm species were identified by resonance Raman spectroscopy as the ferrous oxy (A) (44) and oxoferryl (F) (45) intermediates, respectively. It was reported that during the reaction of the R enzyme with O₂, A decays directly into F without any in-between intermediate (38, 39).

In this work, we studied the reaction of the R cytochromes *bd* from *Escherichia coli* and *Azotobacter vinelandii* with oxygen, using the flow-flash method by means of spectroscopic and electrometric techniques that allow the recording of absorption spectra and membrane potential development with 1-μs time resolution. We were able to detect a transient formation of a spectrally discernible intermediate between A and F.

* This work was supported by grants from Biocentrum Helsinki, the Sigrid Juselius Foundation, the Academy of Finland, the Russian Foundation for Basic Research (Project 05-04-48096), Howard Hughes Medical Institute (Project 55005615), and the Civilian Fund for Research and Development (Project RUB-1-2836-MO-06). The costs of publication of this article were defrayed in part by the payment of page charges. This article must therefore be hereby marked “advertisement” in accordance with 18 U.S.C. Section 1734 solely to indicate this fact.

[†] Both authors contributed equally to this work.

[‡] To whom correspondence should be addressed. Tel.: 358-9-19158005; Fax: 358-9-19159920; E-mail: michael.verkhovsky@helsinki.fi.

³ The abbreviations used are: O, fully ferric species; A, ferrous oxy species; P, peroxy species; F, oxoferryl species; R, fully ferrous species; τ, time constant, reciprocal of rate constant; CCo, cytochrome *c* oxidase; MOPS, 4-morpholinepropanesulfonic acid.

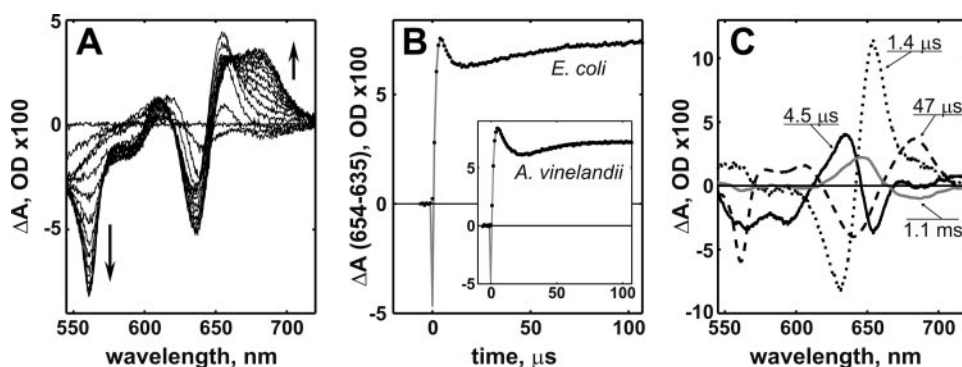


FIGURE 1. Reaction of the fully reduced cytochrome *bd* with oxygen at +21 °C. **A**, absorbance time-wavelength surface of optical changes after flash-induced dissociation of CO from the *E. coli* enzyme in the presence of O₂. Shown are the selected spectra taken at 0, 1, 2, 3, 5, 9 μs, and further in 10-μs increments. The direction of signal development in time is indicated by arrows. **B**, time courses of the reaction at 654–635 nm with cytochromes *bd* from *E. coli* (main panel) and *A. vinelandii* (inset). The theoretical curve (gray solid line) to the data (dots) gives unresolved CO photolysis (*R*-CO → *R*) followed by three exponentials with time constants of 1.4 (1.6) μs (*R* → *A*), 4.5 (9.7) μs (*A* → *P*), and 47 (20.4) μs (*P* → *F*). The τ values in parentheses refer to the *A. vinelandii* enzyme. **C**, kinetic difference spectra of the 1.4-μs (dotted line), 4.5-μs (solid line), 47-μs (dashed line), and 1.1-ms (gray solid line) phases in the visible spectral region. Conditions were: enzyme, 8.8 μM; O₂, 365 μM; CO, 0.5%; Mops-KOH, 65 mM; phosphate-KOH, 35 mM (pH 7.0); sodium ascorbate, 1.25 mM; *N,N,N',N'*-tetramethyl-1,4-phenylenediamine, 2.5 μM; and either *N*-lauroyl-sarcosine, 0.05% (the *E. coli* enzyme) or dodecyl-β-D-maltoside, 0.02% (the *A. vinelandii* enzyme); all concentrations after 1:1 mixing; optical path, 1 cm. For other conditions, see "Experimental Procedures."

EXPERIMENTAL PROCEDURES

Carbon monoxide, oxygen, nitrogen, and argon gases were from AGA; plant L-lecithin was from Avanti Polar Lipids (Alabaster, AL). Other basic chemicals and biochemicals were from Sigma-Aldrich, Merck, Anatrace, Fluka, and Serva.

E. coli cells were obtained from GO105/pTK1 strain according to Ref. 46, and cytochrome *bd* oxidase was isolated from cell membranes as described (37, 47). Cytochrome *bd* from *A. vinelandii* strain MK8 was isolated as reported in Ref. 48. Concentration of the enzymes from *E. coli* and *A. vinelandii* was determined from the dithionite-reduced minus as isolated difference absorption spectra using $\Delta\epsilon_{628-607}$ of 10.8 mM⁻¹ cm⁻¹ (33) and $\Delta\epsilon_{628-605}$ of 9.5 mM⁻¹ cm⁻¹ (49), respectively.

Time-resolved Spectrophotometric Measurements—Time-resolved spectrophotometric measurements were performed using a home-built CCD-based instrument. The setup allows acquiring absorption change surfaces with a time resolution of 1 μs between the spectra. Details of the methodology can be found in Ref. 50. To obtain the CO complex of the *R* enzyme, the as-isolated enzyme was (i) deoxygenated by argon equilibration, (ii) reduced under anaerobic conditions with 2.5 mM sodium ascorbate and 5 μM *N,N,N',N'*-tetramethyl-1,4-phenylenediamine, and (iii) equilibrated with 1% CO. The *R*-CO enzyme was transferred to the stopped flow module in a gas-tight Hamilton syringe preflushed with argon and then mixed with oxygen. CO photolysis was initiated by a laser flash (Brilliant B; Quantel, Les Ulis, France; frequency-doubled YAG, 532 nm; pulse energy, 120 mJ).

Time-resolved Measurement of Electric Potential Generation—Reconstitution of cytochrome *bd* into liposomes, the anaerobic sample preparation, and time-resolved electrometric measurements were made as reported (Refs. 37, 39 and references therein).

Software for Experiments and Data Analysis—Instrumental software for experimental setups was written by Dr. N. Belevich

(Helsinki, Finland). MATLAB (The Mathworks, South Natick, MA) was used for data analysis and presentation.

RESULTS

Four Sequential Steps of the Catalytic Cycle—The flow-flash method is a powerful tool for the study of terminal oxidases (51). We used this approach to examine the reaction of cytochrome *bd* oxidases from *E. coli* and *A. vinelandii* in the *R* state with oxygen on the microsecond time scale at +21 °C. To resolve the transient formation and decay of the reaction intermediates, we recorded the optical changes with a time resolution of 1 spectrum/μs. The spectra on Fig. 1A show the development of the optical changes during the first 100 μs of the reaction with the *E. coli* enzyme. The changes at

560, 595, and in the range of 630–680 nm indicate that all of the three hemes, *b*₅₅₈, *b*₅₉₅, and *d*, are involved in this reaction. Fig. 1B shows a time course of the absorbance changes at 654–635 nm. The kinetic behavior at the selected pair of wavelengths clearly shows all sequential phases, because each next phase has an opposite direction of the signal development. The initial unresolved decrease of absorbance reflects the photolysis of CO from the reduced enzyme (*R*-CO → *R* transition) and is followed by the three more transitions that can be well resolved. Global analysis of the surface of the spectra reveals that these transitions can be fitted as three sequential steps with time constants of 1.4, 4.5, and 47 μs (Fig. 1B, main panel) and the corresponding kinetic difference spectra can be obtained (Fig. 1C). The spectrum of the 1.4-μs phase has a trough at 630 nm and a peak at 654 nm (Fig. 1C, dotted line), which is typical of O₂ binding to ferrous heme *d* (52). Thus, the 1.4-μs phase can be clearly assigned to the formation of the *A* intermediate (*R* → *A* transition). It has to be noted that the rate of the *A* formation ($\tau = 1.4 \mu\text{s}$ at [O₂] = 365 μM) linearly depends on the concentration of O₂ (data not shown; see also Refs. 38, 49).

The spectrum of the 4.5-μs phase shown in Fig. 1C (solid line) has a minimum at 654 nm (decay of the *A* intermediate) and a maximum at 635 nm that reflects the formation of an intermediate that has not been resolved in earlier studies (38, 39). We denote this new reaction intermediate as *P* and the 4.5-μs phase as the *A* → *P* transition. The rate of the *P* formation does not depend on the concentration of O₂. The spectrum of the 47-μs phase (Fig. 1C, dashed line) has troughs at 561 nm (due to the oxidation of heme *b*₅₅₈) and at 640 nm (decay of the *P* intermediate) and a peak at 680 nm. The 680-nm peak is diagnostic of the heme *d* oxoferryl species (*F*) (45); thus, the 47-μs phase corresponds to the *P* → *F* transition.

As shown in the inset of Fig. 1B, the oxygen-induced absorption changes of the *A. vinelandii* cytochrome *bd* are very similar to those of the *E. coli* enzyme. With the *A. vinelandii* enzyme,

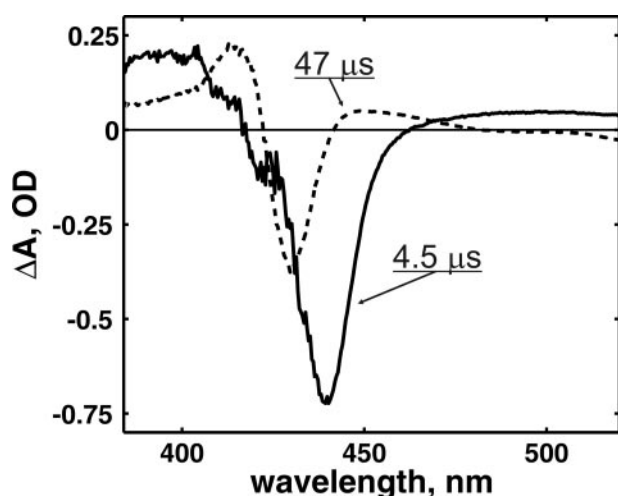


FIGURE 2. Kinetic difference spectra of the 4.5- μ s (solid line) and 47- μ s (dashed line) reaction phases in the Soret spectral region. Conditions were as for Fig. 1.

the apparent time constants for the $R \rightarrow A$, $A \rightarrow P$, and $P \rightarrow F$ transitions are 1.6, 9.7, and 20.4 μ s, respectively.

Because cytochrome *bd* carries the three redox groups, it is three electron-reduced in the *R* state. The reaction of the three electron-reduced enzyme with oxygen stalls at the *F* state, as expected (38, 39). However, under specific conditions of the enzyme isolation, it is possible to purify cytochrome *bd* from *E. coli* that retains some quantity of bound quinol (37). Such a reduced enzyme contains five reducing equivalents, and the O_2 reaction proceeds beyond *F*. Our experiments with this enzyme preparation show an additional phase with $\tau = 1.1$ ms. The spectrum of the 1.1-ms phase has a minimum at 680 and a maximum at 645 nm (Fig. 1C, gray solid line) that may be assigned to the conversion of *F* to the oxidized enzyme (*O*) or more likely into the oxy complex (*A*) because bound quinol is a two electron donor.

The Role of the Heme Groups in the Formation of the Catalytic Cycle Intermediates—When the complex of the ferrous heme *d* with oxygen forms ($R \rightarrow A$ transition), the *b*-type hemes remain reduced, as evidenced by the lack of the distinct troughs at 560 and 595 nm in the spectrum of the 1.4- μ s phase (Fig. 1C). In contrast, the spectrum of the 4.5- μ s phase corresponding to the $A \rightarrow P$ transition has minima at 560 and 595 nm, which are typical features of the oxidized-minus-reduced spectrum of heme b_{595} (37, 53, 54). Further support for the conclusion that heme b_{595} gets oxidized during the $A \rightarrow P$ transition comes from the fact that the difference spectrum of the 4.5- μ s phase in the Soret is dominated by the bleaching at 440 nm (Fig. 2, solid line). The 440-nm band was identified as the Soret band of ferrous heme b_{595} (34, 55). Although the heme *d* absorption change also contributes to the Soret difference spectrum, its contribution to the Soret is usually minor compared with a *b*-type heme (56). It is clear that the *P* formation is accompanied by the oxidation of heme b_{595} . At the same time, there is no evidence for the oxidation of heme b_{558} at this stage.

The oxidation of heme b_{558} occurs during the next transition, the $P \rightarrow F$ transition as evidenced by a prominent trough at 561 nm in the spectrum of the 47- μ s phase (Fig. 1C, dashed line).

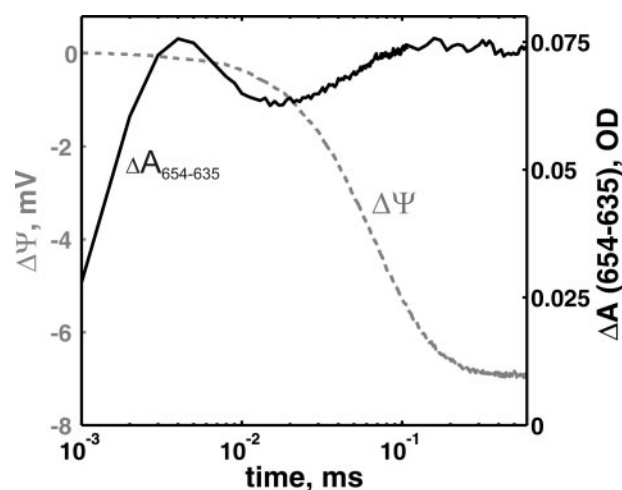


FIGURE 3. Comparison of the electrometric and optical time courses for the reaction of the three electron-reduced *E. coli* cytochrome *bd* with oxygen. Conditions for the electrometric experiment (dashed trace, left axis): Mops-KOH, 100 mM (pH 7.0); *N,N,N',N'*-tetramethyl-1,4-phenylenediamine, 10 μ M; hexaamineruthenium, 10 μ M; glucose, 50 mM; catalase, 0.5 mg/ml; glucose oxidase, 1.5 mg/ml; CO , 1%. Reaction was started by a laser flash after 450 ms from the beginning of injection of 100 μ l of oxygen-saturated buffer ($[O_2] = 1.2$ mM). For the optical experiment (solid trace, right axis), see Fig. 1. All measurements were performed at +21 $^{\circ}C$.

Furthermore, the $P \rightarrow F$ transition is accompanied by a loss of absorbance at 430 nm and its increase at 414 nm (Fig. 2, dashed line). The peaks at 430 and 560 nm were reported to be the Soret and α bands of ferrous heme b_{558} , respectively (29). There is no indication that the oxidation of heme b_{595} , observed during the *P* formation, contributes also to the *F* formation. A trough at 589 nm (Fig. 1C, dashed line) is most probably a specific spectral feature of the compound *F*. A similar feature was observed in the *F*-minus-*O* difference absorption spectrum where *F* was generated by the addition of excess hydrogen peroxide to cytochrome *bd* in the *O* state (41).

The Distribution of the Charge Translocation Events along the Catalytic Cycle—An electrometric recording of the reaction of the fully reduced enzyme from *E. coli* with oxygen is shown in Fig. 3, dashed trace. It consists of an initial non-electrogenic phase (the lag) followed by the electrogenic phase, in agreement with previous reports (37, 39). The fit of the electrometric trace with the rate constants obtained in spectrophotometric measurements revealed that the first two processes, which were assigned to the formation of compound *A* followed by the transition from *A* to *P*, are electrically silent. Thus, both $R \rightarrow A$ and $A \rightarrow P$ transitions are not coupled to any charge translocation across the membrane plane.

In the three electron-reduced cytochrome *bd* (no bound quinol), the electrically silent lag is followed by an electrogenic (Fig. 3, dashed trace) phase that develops concurrently with the 47- μ s phase observed in the spectrophotometric experiment (Fig. 3, solid trace). Thus, it corresponds to the transition of the *P* intermediate to the *F* state ($P \rightarrow F$ transition). When the enzyme contains bound quinol, an additional electrogenic phase with τ of 0.6–1.1 ms is observed. This slow phase matches the corresponding spectral phase reflecting the $F \rightarrow A$ transition (37).

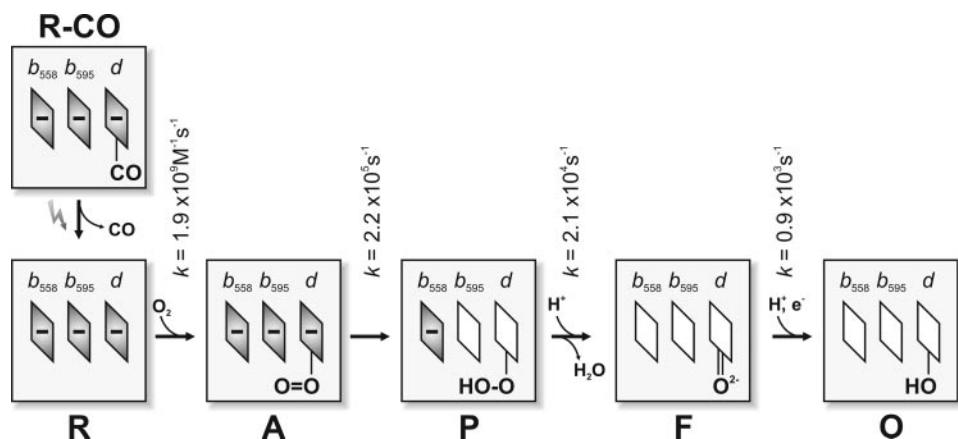


FIGURE 4. **Reaction scheme.** The three rhombuses represent hemes b_{558} , b_{595} , and d , respectively. The minus sign denotes that heme is in the ferrous state. The rate constants refer to the *E. coli* cytochrome *bd*.

DISCUSSION

Why *P* Has Not Been Detected Previously—In this work, we examined the reaction of cytochromes *bd* from *E. coli* and *A. vinelandii* in the **R** state with oxygen. Earlier studies of this reaction reported that the initially formed intermediate **A** decays directly to **F** without any transient intermediate between **A** and **F** (38, 39). This apparently contradicts the identical reaction catalyzed by cytochrome *c* oxidase (CcO), where under the same conditions a transient formation of **P_R** intermediate between **A** and **F** was documented (7). It was concluded that in the reaction of cytochrome *bd* with O_2 there is either no intermediate between **A** and **F** or this intermediate is too short-lived to be detected (39). In this study, we were able to clearly resolve the transient formation of a spectrally discernible intermediate between **A** and **F** with a time constant of 4.5 μs at +21 $^\circ\text{C}$ (Fig. 1), which was denoted **P**. We suggest that **P** was not detected in earlier studies (38, 39) due to some limitations of the methodologies used. In the work of Hill *et al.* (38), the measurements were performed on the appropriate time scale of a few hundred microseconds; however, the measurements were done at selected wavelengths (Fig. 3 in Ref. 38) where the contribution of **P** was small and therefore could not have been trapped. Jasaitis *et al.* (39) tried to catch **P** both in the reaction of the **R** enzyme with O_2 at -20°C and in the reaction of the **O** enzyme with excess H_2O_2 at room temperature. Despite recording the entire spectra, the time resolution (1 ms) appeared to be not sufficient to detect **P** in that study, even at low temperature (39). A question may arise why the **P** formation was not found in the electrometric measurement (39). The present work shows that the initial electrically silent lag phase is actually a sum of the **R** \rightarrow **A** and **A** \rightarrow **P_R** transitions (Fig. 3). This lag phase was also observed in Ref. 39 and compared with the similar lag phase in CcO. It was established that in CcO the lag can be reasonably modeled as two sequential steps corresponding to the **R** \rightarrow **A** and **A** \rightarrow **P_R** transitions (15). Based on the fact that the lag in cytochrome *bd* is markedly shorter than that in CcO, the former was fitted as a single step (39). However, it was not taken into consideration that binding of O_2 to cytochrome *bd* (**R** \rightarrow **A** transition) is ~ 10 times faster compared with CcO (38, 57). Much faster **R** \rightarrow **A** transition in the *bd* oxidase obviously reduces the entire non-electrogenic lag in cytochrome *bd*.

When such a correction with the O_2 on-rates is introduced into analysis, the lag in cytochrome *bd* also must be fitted as two sequential non-electrogenic phases (Fig. 3).

Identity of *P*—In the course of the reaction of the reduced cytochrome *bd* with O_2 , compound **A** decays to an intermediate with a maximum at 635 nm (denoted **P**) with $\tau = 4.5 \mu\text{s}$ (Fig. 1). The **A** \rightarrow **P** transition coincides with the oxidation of heme b_{595} (Figs. 1C and 2). Reduction of O_2 by two electrons is sufficient to generate a two electron-reduced form of O_2 at the active site, *i.e.* bound (hydro)peroxide. It is not

clear, however, whether the O-O bond is broken at this stage of the reaction. If the O-O bond is still intact, **P** corresponds to compound 0 in peroxidases, *i.e.* a true peroxy complex ($\text{Fe}_d^{3+} - \text{O}-\text{O}-(\text{H})$). Compound 0 was monitored in horseradish peroxidase at subzero temperatures (2). Although an intermediate analogous to compound 0 was postulated for CcO, it has never been trapped.

If the O-O bond is already broken, **P** is an oxoferryl species. Formation of the oxoferryl species requires four electrons to break the O-O bond. In the **P** state, two electrons may be taken from heme d and one from heme b_{595} . However, the fourth electron cannot be taken from heme b_{558} because no oxidation of heme b_{558} is observed at this stage (Figs. 1C and 2). Hence, if **P** is oxoferryl, the fourth electron should come from a nearby group, most likely amino acid residue ($\text{Fe}_d^{4+} = \text{O}_2^- \text{R}'$). In the latter case, **P** would be analogous to compound I of cytochrome *c* peroxidase or **P_M** species of CcO. However, withdrawal of an electron from an amino acid residue requires rather high redox potential, typically higher than +0.8 V (58), and the oxidation of heme b_{558} ($E_m \sim +0.15 \text{ V}$) (27) would be much more favorable ($\sim 0.65 \text{ V}$ potential difference, or 10 orders difference in the equilibrium constant). At the same time, in our experiments the formation of **P** is not coupled to the oxidation of the low spin heme, in contrast to that detected during the formation of the **P_R** oxoferryl species in heme-copper oxidases. The oxidation of the low spin heme b_{558} is observed only during decay of **P**, *i.e.* in the next transition. This is the reason why we suggest that in the case of cytochrome *bd* **P** is a true peroxy intermediate. Nevertheless, some further studies are required to establish its precise chemical structure.

Reaction Scheme—The scheme describing the reaction reported in this work is shown in Fig. 4. The initial complex of the **R** cytochrome *bd* with CO (**R-CO**) is photolyzed in the presence of oxygen. The unliganded **R** enzyme generated by the photolysis binds O_2 very rapidly, forming the ferrous heme *d* oxy species (**A**). The **R** \rightarrow **A** transition is not electrogenic, and its rate is proportional to $[\text{O}_2]$ ($k_{\text{on}} = 1.9 \times 10^9 \text{ M}^{-1} \text{ s}^{-1}$) (38, 49). The **A** formation is followed by electron transfer from heme b_{595} to form **P**. The **A** \rightarrow **P** transition occurs with $k = 2.2 \times 10^5 \text{ s}^{-1}$ and is also non-electrogenic. The finding that electron transfer from heme b_{595} to heme d is not coupled with

membrane potential generation is fully consistent with a recent study (37). The chemical structure of **P** needs to be established. As depicted in the scheme, it is likely that **P** is a peroxy complex of ferric heme *d*. If this is the case, the bound peroxide is likely not in the anionic form but at least singly protonated. The proton may come from one of the two protonatable groups linked to the *b*₅₉₅/*d* binuclear site (37) upon its oxidation. We cannot exclude, however, that at the **P** state the O-O bond is already broken and **P** could be similar to **P_M** in CcO. The latter would be apparently inconsistent with the same reaction catalyzed by the **R** CcO where no **P_M**-like intermediate preceding the formation of **P_R** has been observed (7, 16, 17). The **P** intermediate is further converted into **F** with $k = 2.1 \times 10^4 \text{ s}^{-1}$. This is accompanied by the oxidation of heme *b*₅₅₈. In agreement with previous studies (37, 39), formation of **F** is coupled to generation of a membrane potential. There is no doubt that at the **F** state the *b*-type hemes are in the ferric state and heme *d* is in the oxoferryl state. When cytochrome *bd* contains bound quinol, the reaction proceeds further to form the oxidized enzyme (**O**). The **F** → **A** transition occurs with $k = 0.9 \times 10^3 \text{ s}^{-1}$ (Fig. 1C, gray solid line) and is electrogenic (37).

The fact that in the course of the reaction the oxidation of heme *b*₅₉₅ precedes that of heme *b*₅₅₈ may indicate that heme *b*₅₉₅ is located closer to heme *d* than heme *b*₅₅₈. This is in line with the proposal of physical proximity of hemes *d* and *b*₅₉₅ and their functional cooperation in the O₂-reducing site (31–37).

Because an intermediate spectrally and kinetically very similar to **P** of the *E. coli* cytochrome *bd* is also observed with the *bd* enzyme from *A. vinelandii*, **P** is most likely a catalytic intermediate inherent in all members of the *bd*-family of terminal oxidases.

Acknowledgments—We thank Dr. R. B. Gennis and Dr. R. K. Poole for their generous gift of the bacterial strains *E. coli* GO105/pTK1 and *A. vinelandii* MK8, respectively. V. B. B. thanks Dr. A. A. Konstantinov for invaluable help, support, and many stimulating discussions.

REFERENCES

- Jones, P., and Dunford, H. B. (2005) *J. Inorg. Biochem.* **99**, 2292–2298
- Baek, H. K., and Van Wart, H. E. (1989) *Biochemistry* **28**, 5714–5719
- Shintaku, M., Matsuura, K., Yoshioka, S., Takahashi, S., Ishimori, K., and Morishima, I. (2005) *J. Biol. Chem.* **280**, 40934–40938
- Han, S., Ching, Y.-C., and Rousseau, D. L. (1990) *Nature* **348**, 89–90
- Hill, B. C. (1991) *J. Biol. Chem.* **266**, 2219–2226
- Hill, B. C. (1994) *J. Biol. Chem.* **269**, 2419–2425
- Morgan, J. E., Verkhovsky, M. I., and Wikstrom, M. (1996) *Biochemistry* **35**, 12235–12240
- Kitagawa, T., and Ogura, T. (1997) *Prog. Inorg. Chem.* **45**, 431–479
- Proshlyakov, D. A., Pressler, M. A., and Babcock, G. T. (1998) *Proc. Natl. Acad. Sci. U. S. A.* **95**, 8020–8025
- Gennis, R. B. (1998) *Biochim. Biophys. Acta* **1365**, 241–248
- Fabian, M., Wong, W. W., Gennis, R. B., and Palmer, G. (1999) *Proc. Natl. Acad. Sci. U. S. A.* **96**, 13114–13117
- Proshlyakov, D. A., Pressler, M. A., DeMaso, C., Leykam, J. F., DeWitt, D. L., and Babcock, G. T. (2000) *Science* **290**, 1588–1591
- Takahashi, S., Ching, Y.-c., Wang, J., and Rousseau, D. L. (1995) *J. Biol. Chem.* **270**, 8405–8407
- Greenwood, C., Wilson, M. T., and Brunori, M. (1974) *Biochem. J.* **137**, 205–215
- Jasaitis, A., Verkhovsky, M. I., Morgan, J. E., Verkhovskaya, M. L., and Wikstrom, M. (1999) *Biochemistry* **38**, 2697–2706

- Morgan, J. E., Verkhovsky, M. I., Palmer, G., and Wikstrom, M. (2001) *Biochemistry* **40**, 6882–6892
- Karpefors, M., Adelroth, P., Namslaue, A., Zhen, Y., and Brzezinski, P. (2000) *Biochemistry* **39**, 14664–14669
- Sucheta, A., Szundi, L., and Einarsson, O. (1998) *Biochemistry* **37**, 17905–17914
- Brzezinski, P. (2004) *Trends Biochem. Sci.* **29**, 380–387
- Brunori, M., Giuffre, A., and Sarti, P. (2005) *J. Inorg. Biochem.* **99**, 324–336
- Hosler, J. P., Ferguson-Miller, S., and Mills, D. A. (2006) *Annu. Rev. Biochem.* **75**, 165–187
- Iwaki, M., Puustinen, A., Wikstrom, M., and Rich, P. R. (2006) *Biochemistry* **45**, 10873–10885
- Yoshikawa, S., Muramoto, K., Shinzawa-Itoh, K., Aoyama, H., Tsukihara, T., Ogura, T., Shimokata, K., Katayama, Y., and Shimada, H. (2006) *Biochim. Biophys. Acta* **1757**, 395–400
- Borisov, V. B., Forte, E., Sarti, P., Brunori, M., Konstantinov, A. A., and Giuffre, A. (2007) *Biochem. Biophys. Res. Commun.* **355**, 97–102
- Poole, R. K., and Cook, G. M. (2000) *Adv. Microb. Physiol.* **43**, 165–224
- Anraku, Y., and Gennis, R. B. (1987) *Trends Biochem. Sci.* **12**, 262–266
- Junemann, S. (1997) *Biochim. Biophys. Acta* **1321**, 107–127
- Mogi, T., Tsubaki, M., Hori, H., Miyoshi, H., Nakamura, H., and Anraku, Y. (1998) *J. Biochem. Mol. Biol. Biophys.* **2**, 79–110
- Borisov, V. B. (1996) *Biochemistry (Mosc.)* **61**, 565–574
- Puustinen, A., Finel, M., Haltia, T., Gennis, R. B., and Wikstrom, M. (1991) *Biochemistry* **30**, 3936–3942
- Hill, J. J., Alben, J. O., and Gennis, R. B. (1993) *Proc. Natl. Acad. Sci. U. S. A.* **90**, 5863–5867
- Tsubaki, M., Hori, H., Mogi, T., and Anraku, Y. (1995) *J. Biol. Chem.* **270**, 28565–28569
- Borisov, V., Arutyunyan, A. M., Osborne, J. P., Gennis, R. B., and Konstantinov, A. A. (1999) *Biochemistry* **38**, 740–750
- Vos, M. H., Borisov, V. B., Liebl, U., Martin, J.-L., and Konstantinov, A. A. (2000) *Proc. Natl. Acad. Sci. U. S. A.* **97**, 1554–1559
- Borisov, V. B., Sedelnikova, S. E., Poole, R. K., and Konstantinov, A. A. (2001) *J. Biol. Chem.* **276**, 22095–22099
- Borisov, V. B., Liebl, U., Rappaport, F., Martin, J.-L., Zhang, J., Gennis, R. B., Konstantinov, A. A., and Vos, M. H. (2002) *Biochemistry* **41**, 1654–1662
- Belevich, I., Borisov, V. B., Zhang, J., Yang, K., Konstantinov, A. A., Gennis, R. B., and Verkhovsky, M. I. (2005) *Proc. Natl. Acad. Sci. U. S. A.* **102**, 3657–3662
- Hill, B. C., Hill, J. J., and Gennis, R. B. (1994) *Biochemistry* **33**, 15110–15115
- Jasaitis, A., Borisov, V. B., Belevich, N. P., Morgan, J. E., Konstantinov, A. A., and Verkhovsky, M. I. (2000) *Biochemistry* **39**, 13800–13809
- Lorenz, R. M., and Gennis, R. B. (1989) *J. Biol. Chem.* **264**, 7135–7140
- Borisov, V., Gennis, R., and Konstantinov, A. A. (1995) *Biochem. Mol. Biol. Int.* **37**, 975–982
- Borisov, V. B., Gennis, R. B., and Konstantinov, A. A. (1995) *Biochemistry (Mosc.)* **60**, 231–239
- Borisov, V. B., Forte, E., Sarti, P., Brunori, M., Konstantinov, A. A., and Giuffre, A. (2006) *FEBS Lett.* **580**, 4823–4826
- Kahlow, M. A., Loehr, T. M., Zuberi, T. M., and Gennis, R. B. (1993) *J. Am. Chem. Soc.* **115**, 5845–5846
- Kahlow, M. A., Zuberi, T. M., Gennis, R. B., and Loehr, T. M. (1991) *Biochemistry* **30**, 11485–11489
- Kayser, T. M., Ghaim, J. B., Georgiou, C., and Gennis, R. B. (1995) *Biochemistry* **34**, 13491–13501
- Miller, M. J., and Gennis, R. B. (1986) *Methods Enzymol.* **126**, 87–94
- Junemann, S., and Wigglesworth, J. M. (1995) *J. Biol. Chem.* **270**, 16213–16220
- Belevich, I., Borisov, V. B., Bloch, D. A., Konstantinov, A. A., and Verkhovsky, M. I. (2007) *Biochemistry*, in press
- Belevich, I., Bloch, D. A., Belevich, N., Wikstrom, M., and Verkhovsky, M. I. (2007) *Proc. Natl. Acad. Sci. U. S. A.* **104**, 2685–2690
- Gibson, Q., and Greenwood, C. (1963) *Biochem. J.* **86**, 541–555
- Belevich, I., Borisov, V. B., Konstantinov, A. A., and Verkhovsky, M. I. (2005) *FEBS Lett.* **579**, 4567–4570

- 53. Koland, J. G., Miller, M. J., and Gennis, R. B. (1984) *Biochemistry* **23**, 1051–1056
- 54. Lorence, R. M., Koland, J. G., and Gennis, R. B. (1986) *Biochemistry* **25**, 2314–2321
- 55. Zhang, J., Hellwig, P., Osborne, J. P., Huang, H. W., Moenne-Loccoz, P., Konstantinov, A. A., and Gennis, R. B. (2001) *Biochemistry* **40**, 8548–8556
- 56. Poole, R. K. (1988) in *Bacterial Energy Transduction* (Anthony, C., ed), pp. 231–291, Academic Press, London
- 57. Verkhovsky, M. I., Morgan, J. E., and Wikstrom, M. (1994) *Biochemistry* **33**, 3079–3086
- 58. Stubbe, J., and van Der Donk, W. A. (1998) *Chem. Rev.* **98**, 705–762